*Proc. Natl. Acad. Sci. USA*
Vol. 96, pp. 1886–1891, March 1999
Biochemistry

# $tRNA^{Val}$-heterodimeric maxizymes with high potential as gene-inactivating agents: Simultaneous cleavage at two sites in HIV-1 tat mRNA in cultured cells

TOMOKO KUWABARA, MASAKI WARASHINA, AYA NAKAYAMA, JUN OHKAWA, AND KAZUNARI TAIRA*

National Institute for Advanced Interdisciplinary Research, Agency of Industrial Science and Technology, Ministry of International Trade and Industry, Tsukuba Science City 305-8566, Japan; National Institute of Bioscience and Human Technology, Agency of Industrial Science and Technology, Ministry of International Trade and Industry, Tsukuba Science City 305-8562, Japan; and Institute of Applied Biochemistry, University of Tsukuba, Tennoudai 1-1-1, Tsukuba Science City 305-8572, Japan

*Edited by Sidney Altman, Yale University, New Haven, CT, and approved December 21, 1998 (received for review September 14, 1998)*

**ABSTRACT** **It has been demonstrated that shortened forms of (stem II-deleted) hammerhead ribozymes with low intrinsic activity form very active dimers with a common stem II (very active short ribozymes capable of forming dimers were designated maxizymes). Intracellular activities of heterodimeric maxizymes and conventional ribozymes, under the control of a human $tRNA^{Val}$-promoter, were compared against the cleavage of HIV-1 tat mRNA. The pol III-driven maxizymes formed very active heterodimers, and they successfully cleaved HIV-1 tat mRNA in mammalian cells at two sites simultaneously. The cleaved fragments were identified directly by Northern blotting analysis. Despite the initial concerns that a complicated dimerization process and formation of inactive homodimers were involved in addition to the process of association with the target, the overall intracellular activities of $tRNA^{Val}$-driven maxizymes were significantly higher in mammalian cells than those of two sets of independent, conventional hammerhead ribozymes that were targeted at the same two sites within HIV-1 tat mRNA. Because the $tRNA^{Val}$-driven maxizymes tested to date have been more effective than $tRNA^{Val}$-driven "standard" hammerhead ribozymes, the $tRNA^{Val}$-driven heterodimeric maxizymes appear to have potential utility as gene-inactivating agents.**

Hammerhead ribozymes catalyze the sequence-specific cleavage of RNA (1). Ribozymes, including hammerheads (Fig. 1*A*), are metalloenzymes, and their mechanism of action is being clarified (ref. 2 and references therein). For the development of chemically synthesized ribozymes as potential therapeutic agents, attempts were made to remove any surplus nucleotides that are not essential for catalytic activity, leading to the production of initial minizymes, namely, conventional hammerhead ribozymes with a deleted stem/loop II region (3–6). However, the activities of the initial minizymes were two to three orders of magnitude lower than those of the parental hammerhead ribozymes, and it seemed that minizymes might not be suitable as gene-inactivating agents (3–6).

In previous studies (7), it was found that some short ribozymes (Fig. 1*B*) have high cleavage activity that is similar to that of the wild-type parental hammerhead ribozyme (Fig. 1*A*). It was demonstrated that these active species formed dimeric structures with a common stem II, as shown in Fig. 1*B*. To distinguish monomeric forms of conventional minizymes that have extremely low activity from our dimers with high-level activity, the latter, very active, short ribozymes capable of forming dimers are designated "maxizymes" (8). Heterodimeric maxizymes then were designed that only can form binding sites complementary to the substrate sequence when the individual maxizymes form heterodimers. It later was demonstrated *in vitro* that such heterodimeric maxizymes, because of their two independent catalytic cores, could cleave HIV-1 tat mRNA (Fig. 1*C*) at two independent sites simultaneously (9). It also was found that increases in the length of the common stem II were associated with increases in the activity of heterodimeric maxizymes *in vitro*. This is probably because maxizymes with larger numbers of base pairs in the common stem II formed a larger proportion of active heterodimers (Fig. 1 *D* and *E*) whereas, in the case of 2-bp heterodimeric maxizymes (Fig. 1*D*), the dimers were expected to generate a mixture of (2L·2L)-homodimers (consisting of two identical forms of maxizyme left with 2 base pairs in the common stem II), (2R·2R)-homodimers (consisting of two identical forms of maxizyme right), and the desired (2L·2R)-heterodimers (consisting of maxizyme left and maxizyme right). It is partly because of this mixed population of dimers that the activity of 2-bp maxizymes was so low *in vitro* as compared with that of 5-bp maxizymes. However, other studies demonstrated that the strand displacement activity of the cationic detergent cetyltrimethylammonium bromide enhanced the conversion of inactive misfolded maxizymes to active appropriately folded forms (A.N., T.K., M.W., and K.T., unpublished work). As a result, even maxizymes with a short common stem II, such as 2-bp dimeric maxizymes, which tend to form inactive structures *in vitro*, were found to have significant activity in the presence of cetyltrimethylammonium bromide, suggesting that they might be useful *in vivo*, in view of the fact that various facilitators of strand displacement reactions are known to exist *in vivo*.

In this study, we embedded two different maxizymes (with 2- or 5-bp common stem II) and also a standard hammerhead ribozyme, separately, in the 3′-modified region of a human gene for $tRNA^{Val}$ so that each could be transcribed by RNA polymerase III (10) because, for the application of these dimeric maxizymes to gene therapy for the treatment of infectious diseases, such as AIDS, it is important that the maxizymes be expressed constitutively and under the control of a strong promoter *in vivo*. Our $tRNA^{Val}$-expression system enables the transcribed $tRNA^{Val}$-enzyme to be transported from the nucleus to the cytoplasm, thereby ensuring colocalization of the $tRNA^{Val}$-ribozyme with its target mRNA (8, 11). The colocalization of ribozymes and their target RNAs is a major determinant of high-level activity of ribozymes *in vivo* (12, 13). Indeed, this strategy yielded ribozymes that were very active in cultured cells (11, 14), and we also demonstrated that the attached $tRNA^{Val}$-portion does not cause severe steric hindrance during the formation of a dimer (8, 15).

We demonstrate in this paper that the $tRNA^{Val}$-embedded heterodimeric maxizymes had strong activities, regardless of

The publication costs of this article were defrayed in part by page charge payment. This article must therefore be hereby marked "*advertisement*" in accordance with 18 U.S.C. §1734 solely to indicate this fact.

PNAS is available online at www.pnas.org.

This paper was submitted directly (Track II) to the *Proceedings* office.

Abbreviation: LTR, long terminal repeat.

*To whom reprint requests should be addressed at: Institute of Applied Biochemistry, University of Tsukuba, Tennoudai 1-1-1, Tsukuba Science City 305-8572, Japan. e-mail: taira@nibh.go.jp.

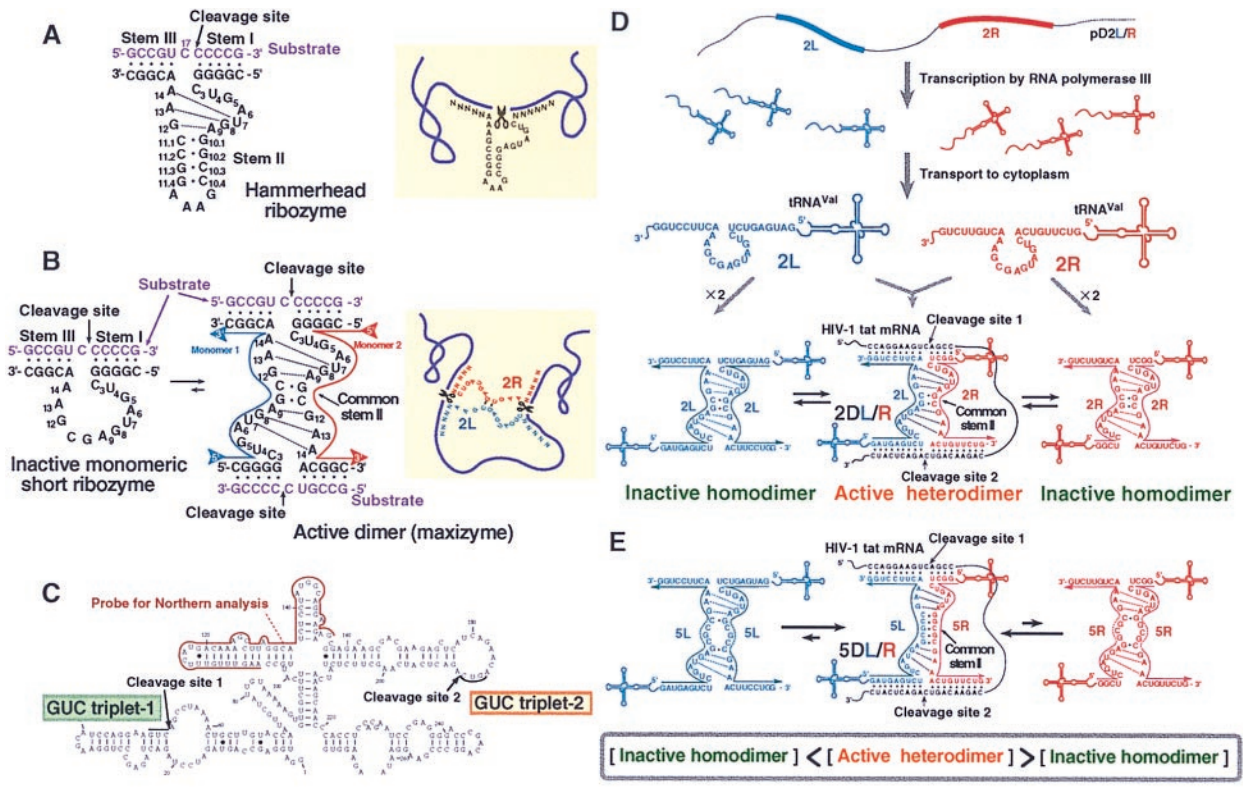


FIG. 1. Secondary structures of (*A*) the wild-type hammerhead ribozyme and (*B*) the minizyme (*Left*) that is capable of forming a homodimer [maxizyme (*Center*)]. All ribozymes were γ-shaped in the crystals, with stems I and II forming the arm of the γ and stem III forming the base and with stem I and stem II being adjacent to each other and stems II and III being stacked colinearly to form a pseudo-A-form helix (2). As shown in *A* by dotted lines, the nucleotides within the catalytic loop form two reversed-Hoogsteen G-A base pairs between $G_8$-$A_{13}$ and $A_9$-$G_{12}$ and a non-Watson–Crick $A_{14}$-$U_7$ base pair that consists of one hydrogen bond. These additional base pairs strengthen the dimeric form of the maxizyme (*B*). The heterodimeric maxizymes can cleave an mRNA at two sites simultaneously (*B Right*). Secondary structure of tat mRNA is shown in *C*. (*D*) The active heterodimeric and inactive homodimeric forms of 2-bp dimeric maxizymes under the control of a human $tRNA^{Val}$-promoter. A large fraction of the population of dimers is expected to be in the inactive homodimeric forms. (*E*) Active heterodimeric and inactive homodimeric forms of the 5-bp dimeric maxizymes. The formation of active forms is favored because perfect base pairing occurs only in the case of active complexes.

the length of the common stem II. To our surprise, the $tRNA^{Val}$-embedded heterodimeric maxizymes were able to reduce the level of HIV-1 tat mRNA more significantly in mammalian cells than could $tRNA^{Val}$-embedded standard hammerhead ribozymes under all sets of conditions that we tested. Therefore, despite the unfavorable dimerization process for the $tRNA^{Val}$-driven maxizymes that are expected to generate a mixture (Fig. 1 *D* and *E*), the $tRNA^{Val}$-driven heterodimeric maxizyme should have significantly higher activity than that of the $tRNA^{Val}$-driven standard ribozyme. Our results indicate that the $tRNA^{Val}$-embedded heterodimeric maxizymes are more active than conventional ribozymes, and they should be powerful candidates for gene-inactivating agents in molecular biology, with potential utility in medicine as well.

## MATERIALS AND METHODS

**Construction of Plasmids for Expression of tRNA-Embedded Enzymes.** Chemically synthesized oligonucleotides encoding maxizyme or the parental hammerhead ribozyme (Fig. 2) and the pol III termination sequence (10) were converted to double-stranded sequences by PCR. After digestion with *Csp*45I and *Sal*I, each appropriate fragment was cloned downstream of the $tRNA^{Val}$ promoter of pUC-dt (which contained the chemically synthesized promoter for a human gene for $tRNA^{Val}$ between the *Eco*RI and *Sal*I sites of pUC 19). The sequences of the constructs were confirmed by direct sequencing.

**Preparation of $tRNA^{Val}$-Enzymes by Transcription.** Ribozyme-expression plasmids p2L, p2R, p5L, p5R, pRz1, and pRz2 (Fig. 3*A*) were used as DNA templates for PCR to construct the DNA templates for transcription. Primers were synthesized for each template, and the sense strand contained the T7 promoter. T7 transcription *in vitro* and purification were performed as described elsewhere (9).

**Kinetic Analysis.** Kinetic parameters of the reactions catalyzed by the $tRNA^{Val}$-enzymes and the so-called nonembedded enzymes were measured with 2 nM 5′-$^{32}$P-labeled short substrate, S19 (5′-CAGAACA**GUC**AGACUCAUC-3′), which included GUC triplet-2 of HIV-1 tat mRNA (Fig. 1*C*). In the assay of Rz1 or N-Rz1 (nonembedded Rz1), which cleaves tat mRNA at GUC triplet-1 (Fig. 1*C*), a second short substrate [S16 (5′-CCAGGAA**GUC**AGCCUA-3′)] was used. Reaction rates were measured, in 25 mM $MgCl_2$ and 50 mM Tris·HCl (pH 8.0), under single-turnover conditions at 37°C (concentrations of enzymes: from 50 nM to 3 μM). The extent of cleavage was determined as described (9).

**Luciferase Assay.** Luciferase activity (Fig. 4) was measured with a PicaGene kit (Toyo-inki, Tokyo) as described elsewhere (16). To normalize the efficiency of transfection by reference to β-galactosidase activity, cells were cotransfected with pSV-β-Galactosidase Control Vector (Promega), and then the chemiluminescent signal caused by β-galactosidase was determined with a luminescent β-galactosidase genetic reporter system (CLONTECH) as described (16).

**Northern Blotting Analysis.** The vectors shown in Fig. 3*A* were used to transfect to long terminal repeat (LTR)–Luc HeLa cells in combination with Lipofectin Reagent (GIBCO/BRL). For the assay of expression of tat mRNA (Fig. 5*B*), pCD-SRα tat (Fig. 4*A*) was used (16, 17). After culture for 36 h at 37°C, total RNA was isolated with ISOGEN (Nippon Gene, Toyama, Japan). For the measurement of the level of HIV-1 tat mRNA (Fig. 5*C*), cells were harvested 8, 20, or 36 h after transfection. Cytoplasmic RNA

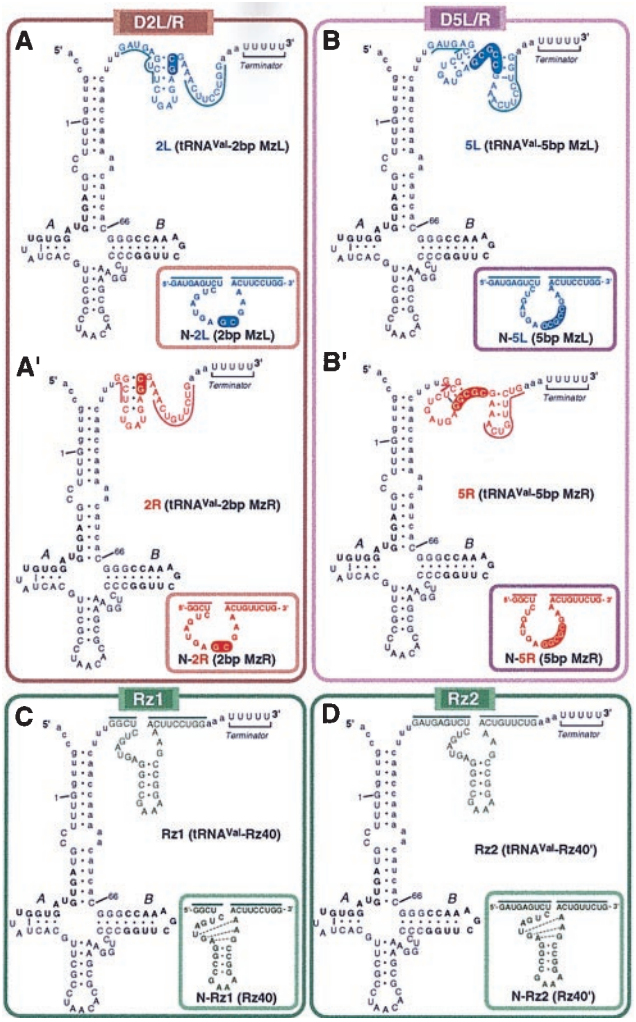


FIG. 2. Predicted secondary structures, based on calculations by the MULFOLD program (Biocomputing Office, Biology Department, Indiana University, Bloomington, IN), of tRNA$^{Val}$-enzymes. The human tRNA$^{Val}$ sequence, including the binding sites of transcription factor TFIIIC (labeled *A* and *B*, corresponding to the A and B box regions), is indicated in uppercase letters with numbering from 1 to 66. Extra sequences that were inserted artificially are indicated by lowercase letters. The sequences of L (maxizyme left) and R (maxizyme right) are shown in blue and red, respectively, and the sequences of standard ribozymes (*C* and *D*) are shown in green. Thick lines indicate the substrate-binding regions of the enzymes. The common stem II regions of the dimeric maxizymes (in *A* and *B*) are indicated by outlined letters within a solid ellipse.

and nuclear RNA were separated as described (18). Thirty micrograms of total RNA per lane (50 $\mu$g for lanes in Fig. 5*C*) were loaded on a 3.0% NuSieve (3:1) agarose gel (FMC), and then bands of RNA were transferred to a Hybond-N nylon membrane (Amersham Pharmacia). The membrane was probed with synthetic oligonucleotides that were complementary to the sequences of respective ribozymes/maxizymes (9). The synthetic probe complementary to the sequence of HIV-1 tat mRNA (indicated in Fig. 1*C*) was used for the determination of the localization and the level of HIV-1 tat mRNA. All probes were labeled with $^{32}$P by T4 polynucleotide kinase (Takara Shuzo, Kyoto).

## RESULTS

**Design of tRNA$^{Val}$-Embedded Maxizymes.** Successful inactivation by ribozymes of a specific gene *in vivo* depends not only on the selection of the target site but also on the design of the expression vector. The latter determines both the level of expression and the half-life of the expressed ribozyme (12, 13). Although pol II promoters might allow tissue-specific or regulatable expression (19), pol III transcripts might be expressed at significantly higher levels (10). High-level expression under control of the pol III promoter clearly would be advantageous if maxizymes

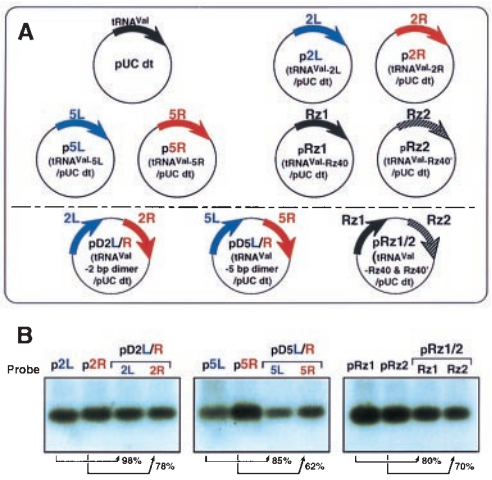


FIG. 3. Schematic representation of the vectors encoding tRNA$^{Val}$-enzymes (*A*) and the levels of expressed tRNA$^{Val}$-enzymes (*B*). When vectors encoding two tRNA$^{Val}$-enzyme cassettes (*A Lower*) had been used to transfect cells, the probes that were complementary to the sequences of respective ribozymes/maxizymes were used independently. The percentage decrease in the level of expression from the vector with two cassettes (*A Lower*), as compared with that from the corresponding vector with one cassette (*A Upper*), is shown by an arrow in each cases.

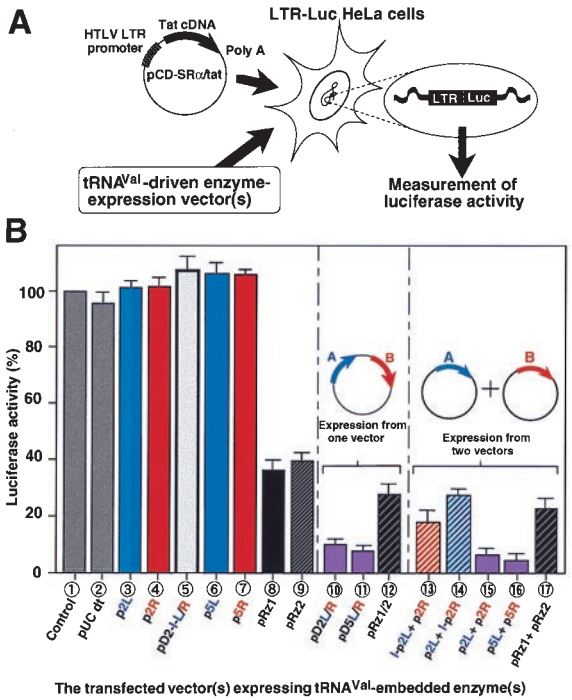


FIG. 4. Intracellular activities of tRNA$^{Val}$-enzymes in LTR-Luc HeLa cells. (*A*) Assay system for measurements of activities of tRNA$^{Val}$-enzymes in LTR-Luc HeLa cells and (*B*) the effects of tRNA$^{Val}$-enzymes on the Tat-mediated transcription of the chimeric LTR-Luc gene. tRNA$^{Val}$-enzyme(s)- and tat-expression vectors were used at a molar ratio of 2:1 for cotransfection of LTR-Luc HeLa cells. The results shown are the averages of results from five sets of experiments. Luciferase activity was normalized by reference to the efficiency of transfection, which was determined by monitoring activity of a cotransfected gene for $\beta$-galactosidase.

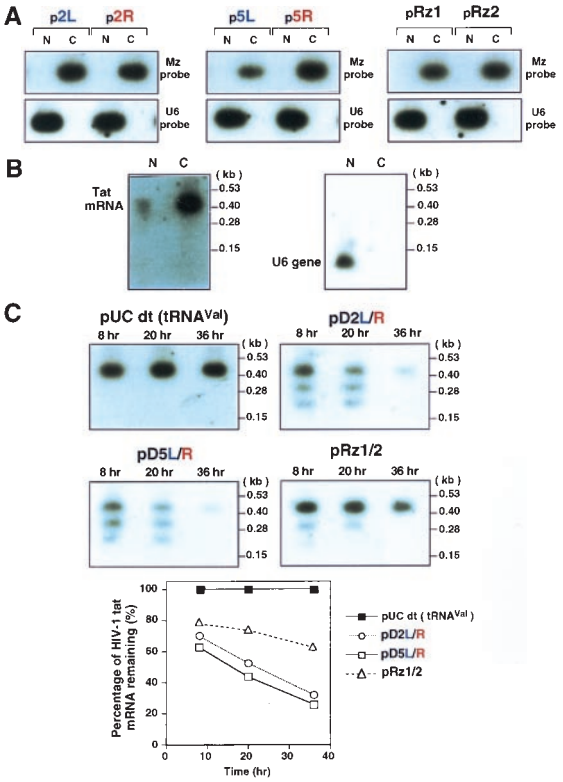


FIG. 5. Intracellular localization of expressed tRNA$^{Val}$-enzymes (*A*) and of tat mRNA (*B*). U6 small nuclear RNA, which remains in the nucleus, was included as a control. Time courses of reductions in levels of HIV-1 tat mRNA by the expressed tRNA$^{Val}$-enzyme(s) also are shown in *C* (calculations were based on densitometric measurements from autoradiograms). N, nuclear fraction; C, cytoplasmic fraction.

are to be used as therapeutic agents and would enhance the likelihood of their dimerization. Therefore, we chose to express our maxizymes under the control of the promoter of a human gene for tRNA$^{Val}$, which previously has been used successfully in the suppression of target genes by ribozymes (13, 14, 20, 21).

The specific design of the tRNA$^{Val}$-embedded enzymes was based on our previous success in attaching a ribozyme sequence to the 3′ modified side of the tRNA$^{Val}$ portion of the human gene to yield very active ribozymes in cultured cells (8, 11, 14, 15). The two different maxizymes, which were targeted to HIV-1 tat mRNA at two sites simultaneously (Fig. 1 *C–E*), were embedded separately in the 3′ modified portion of the tRNA$^{Val}$ sequence (Fig. 2). To compare the activities of the ribozymes in mammalian cells, we used the parental hammerhead ribozymes as controls. These ribozymes are designated Rz40 and Rz40′ in a previous paper (9). As shown in Fig. 2, in the present paper, nonembedded Rz40 and Rz40′ were renamed N-Rz1 and N-Rz2, respectively. They targeted the same cleavage sites (GUC triplet-1 and GUC triplet-2, respectively) as the maxizymes and also were embedded separately in the 3′ modified portion of the tRNA$^{Val}$ sequence (Fig. 2; the tRNA$^{Val}$-embedded standard ribozymes are designated Rz1 and Rz2). In all cases, extra sequences, indicated by lowercase letters in Fig. 2, were inserted, so that (*i*) the transcript would not be processed by pre-tRNA processing enzymes; (*ii*) the structure of the transcript would be sufficiently similar to that of a tRNA to allow recognition by an export receptor for export to the cytoplasm and to ensure colocalization with its target; and (*iii*) the substrate-recognition arms, indicated by underlining in Fig. 2, would avoid formation of stable intramolecular stems so that they would become accessible to the substrate.

**Significant Levels of tRNA$^{Val}$-Enzymes in Mammalian Cells.** In the case of the tRNA$^{Val}$-embedded maxizymes, we were initially worried about the possibility that the tRNA$^{Val}$ portion might cause severe steric hindrance that might inhibit dimerization, with resultant production of monomers with extremely low activity. However, as can be seen in Table 1, the tRNA$^{Val}$-embedded maxizymes retained significant activity. Therefore, we constructed pol III-driven enzyme-expression vectors to examine whether the corresponding transcripts also might be active in mammalian cells. We cloned the maxizymes and the ribozymes downstream of a portion of the gene for tRNA$^{Val}$ (Fig. 3*A*). Because we were also interested in the simultaneous expression of L and R (maxizymes left and right) from one vector, we constructed enzyme-expression vectors that contained both pol III-driven L and R cassettes (Fig. 3*A Lower*, pD2L/R and pD5L/R). For comparison, we also generated the parental hammerhead ribozyme-expression vector, pRz1/2, that contained both pol III-driven Rz1 and Rz2 cassettes.

The relative stabilities in cultured cells of transcripts from these tRNA$^{Val}$-embedded enzyme-expression vectors were estimated by Northern blotting. Transcripts ≈130 nt in length (Fig. 3*B*), which corresponded to the size of the tRNA$^{Val}$-enzymes, were detected in all samples of RNA that we isolated from cultures of LTR-Luc HeLa cells (Fig. 4*A*) that had been transfected separately with each of the plasmids that encoded a tRNA$^{Val}$-enzyme(s) (Fig. 3*A*). As can be seen from Fig. 3*B*, all tRNA$^{Val}$-embedded enzymes were expressed at significant levels in HeLa cells, and all transcripts were obviously stable in these mammalian cells. Levels of transcripts from the expression vectors with a pair of maxizymes or ribozymes (Fig. 3*A Lower*, pD2L/R, pD5L/R, and pRz1/2) were slightly lower than levels of similar transcripts transcribed from two independent vectors [for example, from p2L and p2R (Fig. 3*A Upper*)] (22). Significant levels of expression and colocalization of a transcript with its target are prerequisites for effective ribozymes *in vivo* (see below).

**The Intracellular Activities of tRNA$^{Val}$-Dimeric Maxizymes Were Higher than Those of tRNA$^{Val}$-Standard Hammerhead Ribozymes.** To evaluate the intracellular activities of the tRNA$^{Val}$-embedded dimeric maxizymes and tRNA$^{Val}$-embedded hammerhead ribozymes, we performed the following assay, using LTR-Luc HeLa cells that encoded a chimeric gene that consisted of the LTR of HIV-1 and a gene for luciferase (Fig. 4*A*) (16). The LTR of HIV-1 contains regulatory elements that include a trans-activation responsive element region. The HIV-1 regulatory protein, Tat, binds to TAR, and the binding of Tat stimulates transcription substantially. Therefore, luciferase activity originating from the chi-

Table 1. Kinetic parameters of reactions catalyzed by the tRNA$^{Val}$-embedded enzymes and the corresponding nonembedded enzymes

| | $k_{cat}$, $min^{-1}$ | Apparent $K_M$, $\mu M$ | Apparent $k_{cat}/K_M$, $\mu M^{-1}\cdot min^{-1}$ |
|---|---|---|---|
| tRNA$^{Val}$-embedded enzymes | | | |
| D2L/R | 0.00013 | 0.88 | 0.00015 |
| D5L/R | 0.057 | 0.028 | 2.0 |
| Rz1 | 0.083 | 0.15 | 0.55 |
| Rz2 | 0.065 | 0.13 | 0.50 |
| Nonembedded enzymes | | | |
| N-D2L/R* | 0.006 | 1.0 | 0.006 |
| N-D5L/R* | 0.24 | 0.22 | 1.1 |
| N-Rz1 | 0.85 | 0.040 | 21 |
| N-Rz2 | 0.55 | 0.020 | 28 |

Rate constants were measured, in 50 mM Tris·HCl (pH 8.0) and 25 mM $MgCl_2$, under single-turn over conditions at 37°C. In the assays of Rz1 and N-Rz1, which cleaved HIV-1 tat mRNA at GUC triplet-1 (Fig. 1*C*), a short 16-meric substrate (S16) was used. Except in these two cases, a 19-meric short substrate (S19), which contained GUC triplet-2 of tat mRNA, was used. In the case of maxizymes, the $K_M$ apparent appears to be a complicated quantity, which might roughly characterize the dimerization process (7).
*Kinetic parameters were taken from ref. 9.

meric LTR-Luc gene increases in response to increases in the concentration of Tat (16). Measurements of luciferase activity allowed us to monitor the effects of $tRNA^{Val}$-embedded enzymes on the Tat-mediated transcription of the chimeric LTR-Luc gene. After transient expression of both Tat and $tRNA^{Val}$-embedded enzymes by cotransfection of cells with a tat expression-vector (pCD-SR$\alpha$ tat) and our $tRNA^{Val}$-embedded enzyme-expression vector(s) (Fig. 3*A*), we estimated the intracellular activity of each $tRNA^{Val}$-ribozyme by measuring the luciferase activity.

The luciferase activity recorded when we used only the tat-expressing vector (pCD-SR$\alpha$ tat) was taken as 100%. Enzyme(s)- and tat-expression vectors were used at a molar ratio of 2:1 for cotransfection of LTR-Luc HeLa cells. The results shown are the averages of results from five sets of experiments (Fig. 4*B*). As shown in Fig. 4*B*, all of the $tRNA^{Val}$-dimeric maxizymes were extremely effective (>90% inhibition), despite the fact that the SR$\alpha$ promoter, which controlled the transcription of the target tat mRNA, is 10- to 30-fold more active than the SV40 early promoter regardless of species and origin of cells (17). $tRNA^{Val}$-hammerhead ribozymes were also effective, albeit to a lesser extent (>60% inhibition). Clearly, $tRNA^{Val}$-L and $tRNA^{Val}$-R could be transcribed either from one vector or from two independent vectors, and, in either case, the heterodimers of $tRNA^{Val}$-maxizymes were more active than the standard $tRNA^{Val}$-ribozymes.

To our surprise, the $tRNA^{Val}$-embedded 2-bp dimeric maxizyme [D2L/R (Fig. 4*B*, lanes 10 and 15)], which had very weak activity *in vitro* (Table 1), turned out to have a very strong inhibitory effect in mammalian cells. This result is in accord with our separate finding that, in the presence of various facilitators of strand-displacement reactions that are known to exist *in vivo*, 2-bp dimeric maxizymes are almost as active as 5-bp dimeric maxizymes (A.N., T.K., M.W., and K.T., unpublished work). It is important to note that, because each separate $tRNA^{Val}$-maxizyme [2L, 2R, 5L, and 5R (Fig. 4*B*, lanes 3, 4, 6, and 7)] did not, by itself, have any inhibitory effects, the activities of the $tRNA^{Val}$-embedded maxizymes must have originated from the formation of active heterodimers in mammalian cells. Moreover, because the inactive $tRNA^{Val}$-driven maxizymes (D2-I-L/R and D5-I-L/R) that had been created by a single $G^5$ to $A^5$ mutation within the catalytic core did not show any inhibitory effects (the result for D2-I-L/R is shown in Fig. 4*B*, lane 5; D5-I-L/R also did not show any inhibitory effects), it is clear that the intracellular activities of the $tRNA^{Val}$-embedded ribozymes originated from their cleavage activities in cultured cells and not from the antisense effects. Combination of active and inactive maxizymes demonstrated that each of two catalytic domains was active by itself: Note—for example, in Fig. 4*B*, lane 13—that the combination of the active maxizyme right (2R) and the inactive maxizyme left (I-2L) created a heterodimeric maxizyme with only the half-site active; nevertheless, the resulting half-site active heterodimeric maxizyme had significant activity [indeed, its activity was higher than that of the corresponding parental ribozyme, Rz1 (Fig. 4*B*, lane 8)].

It should be mentioned that, in the case of a specific example of the heterodimeric maxizyme against *BCR-ABL* gene (8), the maxizyme had acted efficiently and specifically not only against the reporter gene construct in HeLa cells (a similar assay system as shown in Fig. 4 was used) but also against an endogenous *BCR-ABL* (b2a2 mRNA) target in $tRNA^{Val}$-maxizyme-stably transduced BaF3/$p210^{BCR\text{-}ABL}$ cells as well as in BV173 cells that were derived from a patient with a Philadelphia chromosome. These observations clearly demonstrate that the absolute levels of the maxizyme transcripts are high enough to promote dimerization process even in maxizyme-stably transduced cells.

**Successful Transport of Expressed $tRNA^{Val}$-Enzymes to the Cytoplasm that Ensured Colocalization with Their Target mRNA and Detection of the Cleavage of HIV-1 tat mRNA in LTR-Luc HeLa Cells.** Because colocalization of a ribozyme with its target is obviously an important determinant of the ribozyme's efficiency *in vivo* (12, 13), it was essential to determine the intracellular localization of our $tRNA^{Val}$-enzymes. Total RNA from LTR-Luc HeLa cells that had been transfected with each expression vector was separated into nuclear and cytoplasmic fractions. Then, levels of each transcribed enzyme were examined by Northern blotting analysis with a probe specific for the maxizyme or ribozyme. As shown in Fig. 5*A* and as expected from the properties of our $tRNA^{Val}$-expression system (11), all $tRNA^{Val}$-embedded enzymes were found in the cytoplasmic fraction, and none were detected to any significant extent in the nuclear fraction. U6 small nuclear RNA, which is known to remain in the nucleus, was included in these studies as a control (Fig. 5*A Lower*). We then investigated the localization of the target tat mRNA in LTR-Luc HeLa cells by Northern blotting with a probe specific for HIV-1 tat mRNA. As shown in Fig. 5*B* and as we had anticipated, we found tat mRNA predominantly in the cytoplasmic fraction. Thus, the $tRNA^{Val}$-driven enzymes were colocalized with the target tat mRNA (Fig. 5*A*).

To confirm directly that the inhibitory effects of the dimeric maxizymes originated from the cleavage of tat mRNA, we performed Northern blotting analysis (Fig. 5*C*). We determined the time courses of the reduction in level of HIV-1 tat mRNA by $tRNA^{Val}$-embedded enzymes. Total RNA from LTR-Luc HeLa cells that had been transfected with the tat-expression plasmid (pCD-SR$\alpha$ tat) and the plasmid encoding each $tRNA^{Val}$-enzyme was extracted 8, 20, and 36 h after transfection. Then, the amount of tat mRNA was determined as shown in Fig. 5*C*. The length of the cleaved fragments was exactly as anticipated (9). We confirmed, by mixing cells producing only the substrate and other cells producing only the enzyme before the isolation of total RNA, that the cleavage of mRNA did not occur during our RNA isolation procedure (8, 23). No reduction in the level of expressed tat mRNA was noted in the case of the control (transfection with pUC dt), and this level of tat mRNA was taken as 100%. As can be seen in the lowest panel of Fig. 5*C*, it is clear that the decrease in the level of tat mRNA was more apparent in cells that produced $tRNA^{Val}$-maxizymes than in those that produced $tRNA^{Val}$-standard ribozymes. These results were in good agreement with the results of the assays of luciferase activity shown in Fig. 4*B*. The heterodimeric maxizymes cleaved the target mRNA

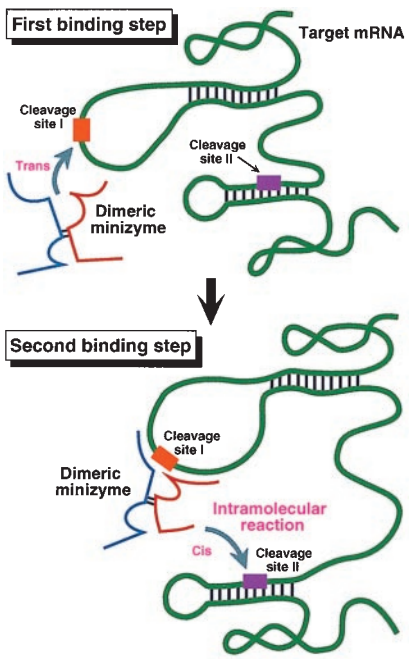


FIG. 6. Schematic representation of the cleavage of an mRNA at two sites by a dimeric maxizyme.

more efficiently, in mammalian cells, than the combination of the two independent standard ribozymes.

## DISCUSSION

When minizymes (stem II-deleted monomeric short ribozymes) first were studied, it appeared that they were significantly less active than the corresponding full-length ribozymes. However, the activities of our dimeric short ribozymes (nonembedded short ribozymes) were found to be equal to those of the parental hammerhead ribozymes despite the smaller sizes of the maxizymes (refs. 7 and 9; very active short ribozymes capable of forming dimers were designated maxizymes). Therefore, theoretically, we should be able to modify nonembedded maxizymes chemically to render them resistant to intracellular RNases for use *in vivo*, as has been achieved in the case of standard hammerhead ribozymes (24). Moreover, we demonstrate in the present study that, for the cleavage of HIV-1 tat mRNA, $tRNA^{Val}$-driven maxizymes formed heterodimeric structures with high-level activity. These maxizymes were more effective than similarly transcribed standard ribozymes in mammalian cells. Moreover, all $tRNA^{Val}$-driven transcripts, including $tRNA^{Val}$-embedded standard ribozymes, were exported efficiently to the cytoplasm for colocalization with their target tat mRNA.

The heterodimers of $tRNA^{Val}$-driven maxizymes cleaved two sites within tat mRNA more efficiently than two independent $tRNA^{Val}$-driven ribozymes, each targeted to one of the two cleavage sites, despite the fact that, in the case of the maxizymes, a complicated dimerization process is involved in addition to the process of association with the target. The activities in mammalian cells of $tRNA^{Val}$-maxizymes (especially for the 2-bp heterodimeric maxizyme D2L/R) relative to those of standard ribozymes (Fig. 4) were greater than we had anticipated from kinetic parameters determined *in vitro* (Table 1). In general, the rate-limiting step of a reaction mediated by a catalytic RNA, such as a ribozyme, *in vivo* has been considered to be the substrate-binding step (12, 13, 25–29). Under such $k_{cat}/K_M$ controlled reaction conditions, once the dimeric maxizyme has bound to the more accessible target site with one of its binding arms (site I in Fig. 6; the interaction at this site has a lower $K_M$ value than that of the other interaction at site II), the subsequent second binding step at the second site becomes an intramolecular interaction. This intramolecular annealing process is entropically more favorable than the intermolecular annealing process in which independent standard ribozymes are involved. [Ribozymes attacking multiple sites are, in general, more efficient in reducing gene expression than ribozymes targeted to one site only (see refs. 30 and 31).] The dual-site maxizymes also might have an off-rate advantage; that is, while one site is displaced by translation or other facilitators of strand displacement, continued binding of another site would keep the RNAs associated, facilitating the rebinding of the displaced site. In other cases, even if the second target site has a high $K_M$ value because of some undesirable tertiary structure of the target mRNA (a hidden target site), the binding at the first site might change the overall structure of the mRNA and the second site might become more accessible. Such phenomena, in addition to the minimal decrease in activity associated with embedding in a tRNA, might contribute to the strong activities of heterodimeric maxizymes in mammalian cells.

The cleavage activity of the $tRNA^{Val}$-driven heterodimeric maxizyme, in particular in cells, should involve a trimolecular interaction (between the two $tRNA^{Val}$-driven monomer units and the target substrate). By contrast, the activity of conventional ribozymes involves a bimolecular interaction (between one $tRNA^{Val}$-driven ribozyme and its target). In principle, bimolecular interactions are more rapid than trimolecular interactions. This difference would seem to indicate that conventional ribozymes might be more effective in cells than $tRNA^{Val}$-driven heterodimeric maxizymes. However, in our experiments, we found that the $tRNA^{Val}$-driven dimer was always more active than the corresponding $tRNA^{Val}$-driven ribozyme when we tested several target sequences in cultured cells (the same target site was used for each set of ribozyme and maxizyme). This conclusion is strengthened further by the results of the present analysis. Therefore, as long as our $tRNA^{Val}$-expression system is used, despite the involvement of the dimerization process, the intracellular activity of the maxizyme appears to be significantly higher than that of conventional hammerhead ribozymes.

In conclusion, although our $tRNA^{Val}$-expression system can produce very active ribozymes (11, 14), in our hands, the corresponding dimeric maxizymes are consistently more active than standard hammerhead ribozymes in mammalian cells (8, 15). Therefore, we encourage molecular biologists to use $tRNA^{Val}$-driven maxizymes in their attempts to suppress the expression of a specific gene of interest. The $tRNA^{Val}$-driven heterodimeric maxizymes, which are capable of cleaving a substrate at two independent sites simultaneously, can be designed very easily and, thus, they should be very useful as tools in molecular biology, with potential use *in vivo* and in a clinical setting.


1. Symons, R. H. (1989) *Trends Biochem. Sci.* **14,** 445–450.
2. Zhou, D.-M. & Taira, K. (1998) *Chem. Rev. (Washington, D.C.)* **98,** 991–1026.
3. McCall, M. J., Hendry, P. & Jennings, P. A. (1992) *Proc. Natl. Acad. Sci. USA* **89,** 5710–5714.
4. Tuschl, T. & Eckstein, F. (1993) *Proc. Natl. Acad. Sci. USA* **90,** 6991–6994.
5. Fu, D. J., Benseler, F. & McLaughlin, L. W. (1994) *J. Am. Chem. Soc.* **116,** 4591–4598.
6. Long, D. M. & Uhlenbeck, O. C. (1994) *Proc. Natl. Acad. Sci. USA* **91,** 6977–6981.
7. Amontov, S. & Taira, K. (1996) *J. Am. Chem. Soc.* **118,** 1624–1628.
8. Kuwabara, T., Warashina, M., Tanabe, T., Tani, K., Asano, S. & Taira, K. (1998) *Mol. Cell* **2,** 617–627.
9. Kuwabara, T., Amontov, S., Warashina, M., Ohkawa, J. & Taira, K. (1996) *Nucleic Acids Res.* **24,** 2302–2310.
10. Perriman, R. & de Feyter, R. (1997) in *Methods in Molecular Biology: Ribozyme Protocols,* ed. Turner, P. C. (Humana, Totowa, NJ), pp. 393–402.
11. Koseki, S., Tanabe, T., Tani, K., Asano, S., Shioda, T., Shimada, T., Nagai, Y., Ohkawa, J. & Taira, K. (1999) *J. Virol.*, in press.
12. Sullenger, B. A. & Cech, T. R. (1993) *Science* **262,** 1566–1569.
13. Bertrand, E., Castanotto, D., Zhou, C., Carbonnelle, C., Lee, G. P., Chatterjee, S., Grange, T., Pictet, R., Kohn, D., Engelke, D., *et al.* (1997) *RNA* **3,** 75–88.
14. Kawasaki, H., Eckner, R., Yao, T.-P., Taira, K., Chiu, R., Livingston, D. M. & Yokoyama, K. K. (1998) *Nature (London)* **393,** 284–289.
15. Kuwabara, T., Warashina, M., Orita, M., Koseki, S., Ohkawa, J. & Taira, K. (1998) *Nat. Biotechnol.* **16,** 961–965.
16. Koseki, S., Ohkawa, J., Yamamoto, R., Takebe, Y. & Taira, K. (1998) *J. Controlled Release* **53,** 159–173.
17. Takebe, Y., Seiki, M., Fujisawa, J., Hoy, P., Yokota, K., Arai, K., Yoshida, M. & Arai, N (1988) *Mol. Cell. Biol.* **8,** 466–472.
18. Huang, Y. & Carmichael, G. G. (1996) *Mol. Cell. Biol.* **16,** 1534–1542.
19. Benedict, C. M., Pan, W., Loy, S. E. & Clawson, G. A. (1998) *Carcinogenesis* **19,** 1223–1230.
20. Baier, G., Coggeshall, K. M., Baier-Bitterlich, G., Giampa, L., Telford, D., Herbert, E., Shih, W. & Altman, A. (1994) *Mol. Immunol.* **31,** 923–932.
21. Yu, M., Leavitt, M. C., Maruyama, M., Yamada, O., Young, D., Ho, A. D. & Wong-Staal, F. (1995) *Proc. Natl. Acad. Sci. USA* **92,** 699–703.
22. Armentano, D., Yu, D.-F., von Ruden, T., Anderson, W. F. & Gilboa, E. (1987) *J. Virol.* **61,** 1647–1650.
23. Warashina, M., Kuwabara, T., Nakamatsu, Y. & Taira, K. (1999) *Chem. Biol.*, in press.
24. Jarvis, T. C., Wincott, F. E., Alby, L. J., McSwiggen, J. A., Beigelman, L., Gustofson, J., DiRenzo, A., Levy, K., Arthur, M., Matulic-Adamic, J., *et al.* (1996) *J. Biol. Chem.* **271,** 29107–29112.
25. Pontius, B. W. & Berg, P. (1991) *Proc. Natl. Acad. Sci. USA* **88,** 8237–8241.
26. Crisell, P., Thompson, S. & James, W. (1993) *Nucleic Acids Res.* **21,** 5251–5255.
27. Ellis, J. & Rogers, J. (1993) *Nucleic Acids Res.* **21,** 5171–5178.
28. Kronenwett, R., Haas, R. & Sczakiel, G. (1996) *J. Mol. Biol.* **259,** 632–644.
29. Sioud, M. & Jesperson, L. (1997) *J. Mol. Biol.* **257,** 775–789.
30. Ohkawa, J., Yuyama, N., Takebe, Y., Nishikawa, S. & Taira, K. (1993) *Proc. Natl. Acad. Sci. USA* **90,** 11302–11306.
31. Guerrier-Takada, C., Salavati, R. & Altman, S. (1997) *Proc. Natl. Acad. Sci. USA* **94,** 8498–8472.